Table of Contents

DESIGN AND SYNTHESIS OF SUBSTRATE LIKE PEPTIDOMIMETIC INHIBITORS

To design of novel DPP-4 inhibitors ligand based and structure based screening approaches were applied and piperazine based peptidomimetics were screened and evaluate as potent and selective DPP-4 inhibitors for the treatment of T2DM.

4.1 Design of NCE's

In our previous studies, we have built HQSAR model for prediction of selectivity of DPP-4 inhibitors [1] and pharmacophore based 3D-QSAR models and CoMFA/CoMSIA anyalsis [2] for azabicyclo derivatives for prediction of DPP-4 inhibitory activity. To improve the potency as well as selectivity and stability it's required to optimize lead molecules by rational way, in such context fragment based HQSAR modeling were carried out. From the atomic contribution maps obtained using the HQSAR model, it was revealed that ortho or pera electro-withdrawing substituent's on the phenyl ring at S2 site contributed to the inhibition activity. According to this study, in order to obtain selective DPP-4 inhibitors compared to the isozymes, the interaction of the inhibitors with the S2 site and S1 site in DPP-4 should be carefully considered. Docking studies of highly active molecules of azabicyclo series were also performed to explore the binding mode of these molecules into the active site of DPP-4 target [3].

In pharmacophore studies, identified validate pharmacophore model containing two hydrogen bond acceptors (A), Hydrophobic (H), positive (P) and aromatic rings (R).These pharmacophore model further applied to large database screening, hits was the compelling pharmacophoric feature (AAHPR), showing good receptor interaction, structurally similar and having same basic nucleus piperazine as a linker with different substitution at S1 and S2 site. Ligand-based construction of a pharmacophore model, confirmed that the piperazines include an ideal geometry of two essential features required for a good affinity profile: a basic amine (protonated at physiological pH) and a hydrophobic feature. In continuation of above work, Novel lead molecules combinatorial screening was performed using best docked conformation of highly active molecule of piperazine series. Nevertheless, ADMET, HQSAR, pharmacophore modeling and docking studies were used to validate the screened molecules for DPP-4.

To design new chemical entities piperazine was consider as base lead as linker and grow new substituent on both S1 and S2 site [14]. At S1 site consider different five member hetrocyclic ring With h-bond accepto rfeatures like Pyrrole, Pyrazole, Imidazole, Thiazole, Isothiazole, Oxazole, Triazole, Prollidine, Thiazolidine and at S2 site consider different aromaticandhetro-aromatic ring With electronegative features (Pyridine, Pyrimidine, Benzoxazole, Benzthiazole, benimidazole). Taking all combination a combinatorial library of around ~10,000 molecules were generated using Lead grow software (Fig. 4.1) [4]. Further, these molecules were screened at different screening level. First, these were checked for pharmacoric alignment that molecule contain all required feature (AAHPR) and 3D-QSAR based activity. At second level screened molecules were further subjected for selectivity prediction by HQSAR Models. In third level of screening molecule were dock in DPP-4 target active site to explore the biding interaction with three level of precision mode HTVS (High-throughput virtual screening), slandered precision (SP) and Extra precision (XP). As early ADME and toxicity predictions for new molecules are important to reduce the chance of failure of drug candidates during clinical trials. So, *in silico ADME and* toxicity studies were carried out for all the screened molecules. At last stage of designing, outcome screening molecules were visually inspected on basis of literature; medicinal chemistry and synthesis approaches 24 new molecule were designed. In designed molecule piperazine was selected lead and linker between S1 and S2 site groups. At S1 site three main five member ring cynoprolidine, 2 amino thiazole and 4 amino-1,2,4 triazole were selected and At S2 site different aromatic and hetroaromatics containing electronegative group were introduced in order to further expand our exploration and better understand the structure–activity relationships of piperazine derivatives as shown in figure 4.2.

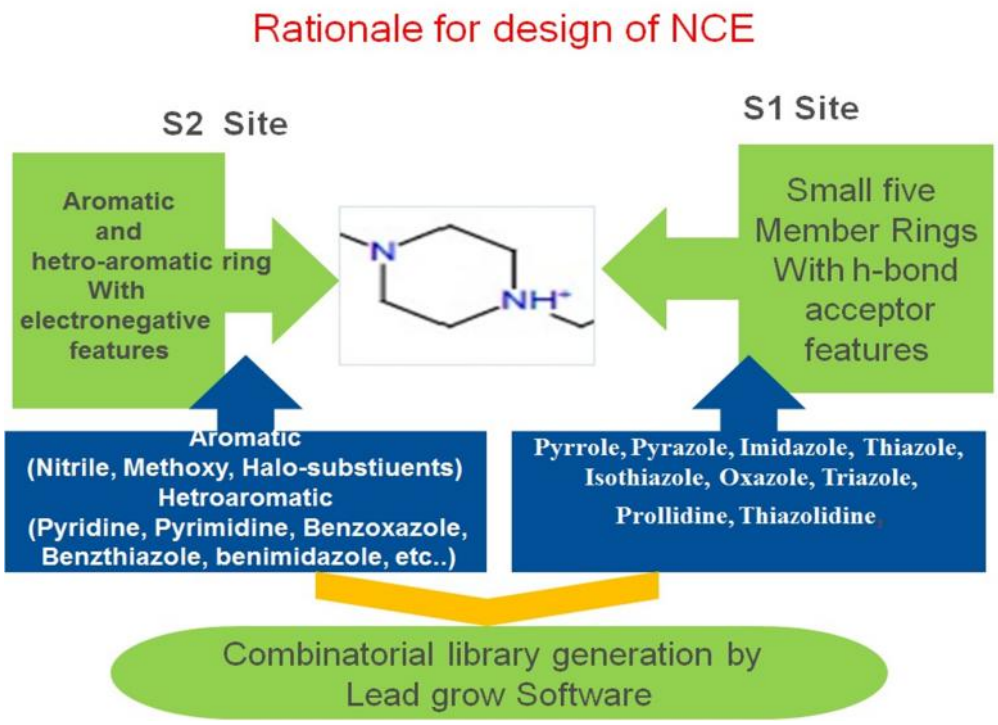

Figure 4.1 Rationale for combinatorial library generation for design of NCE

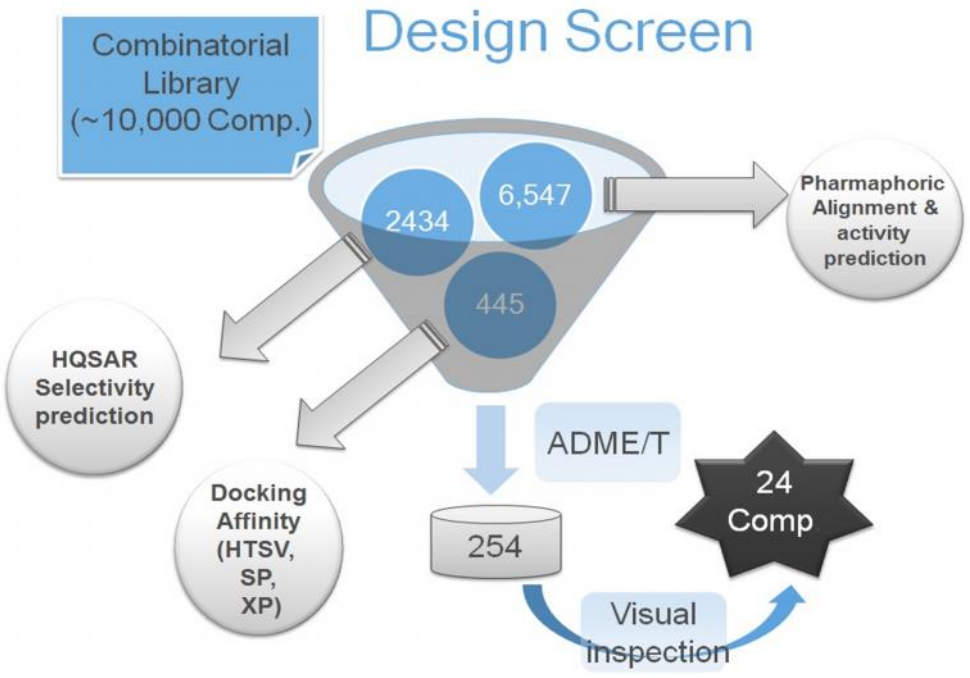

Figure 4.2 Combinatorial library screen work flow

Table 4.1 Predicted activity and pharmacophore alignment score of designed molecules

Compound	Predicted Activity	Fitness Score	No. Site matched
6a	7.48	1.65	5
6b	6.88	1.80	5
6c	7.51	1.93	5
6d	7.02	1.95	5
6e	6.89	1.63	5
6f	7.09	1.91	5
6g	6.87	1.99	5
6h	6.61	1.81	5
10a	6.78	1.59	4
10b	7.19	1.78	4
10c	6.71	1.52	4
10d	6.88	1.52	4
10e	7.09	1.50	4
10f	7.02	1.76	4
10g	6.89	1.74	4
10h	7.09	1.68	4
14a	7.07	1.47	4
14b	6.61	1.57	4
14c	7.18	1.84	4
14d	7.19	1.35	4
14e	6.81	1.58	4
14f	6.88	1.53	4
14g	7.09	1.49	4
14h	7.02	1.60	4

Tables4.2 Selectivity prediction of designed molecules by HQSAR models

Compound	Model A[a]	Model B[b]	Model C[C]
6a	12.55	9.8	12.14
6b	12.3	11.08	10.05
6c	11.43	10.25	10.43
6d	12.53	9.89	10.82
6e	11.34	11.12	10.60
6f	11.70	10.61	11.84
6g	11.51	10.82	11.88
6h	12.12	11.58	11.47

10a	13.86	10.5	12.99
10b	13.60	9.79	10.91
10c	12.74	10.96	11.29
10d	13.84	9.61	11.67
10e	12.65	9.83	11.46
10f	13.01	10.35	12.69
10g	12.81	11.53	12.73
10h	13.42	11.29	12.32
14a	13.65	10.458	13.18
14b	13.39	10.744	11.09
14c	12.53	9.923	11.47
14d	13.62	9.562	11.86
14e	12.43	9.788	11.64
14f	12.79	10.28	12.88
14g	12.60	10.48	12.91
14h	13.21	11.24	12.51

a- Selectivity between DPP-4 and DPP-2
b- Selectivity between DPP-4 and DPP-8
c- Selectivity between DPP-4 and DPP-9

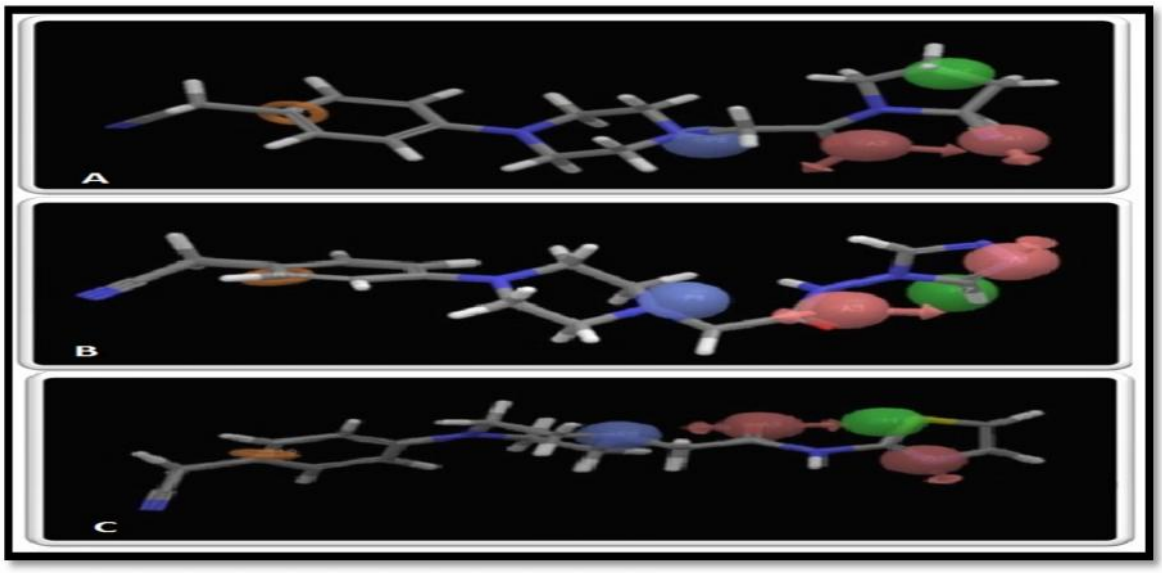

Figure 4.3 (i) pharmacophore feature aligned on designed compound 6a (A) 10a (B) and 14a (C) **3(ii)**Thepharmacophore hypothesis showingdistances between pharmacophoric sites (A) and angles (B)

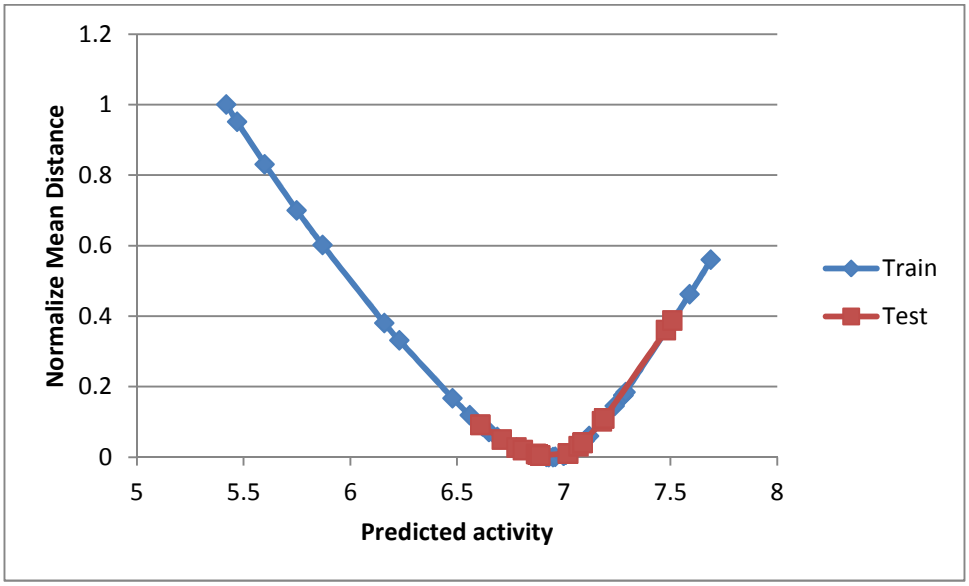

Figure 4.4 Scatter plot between normalized mean distance vs. respective activity of both training and test set

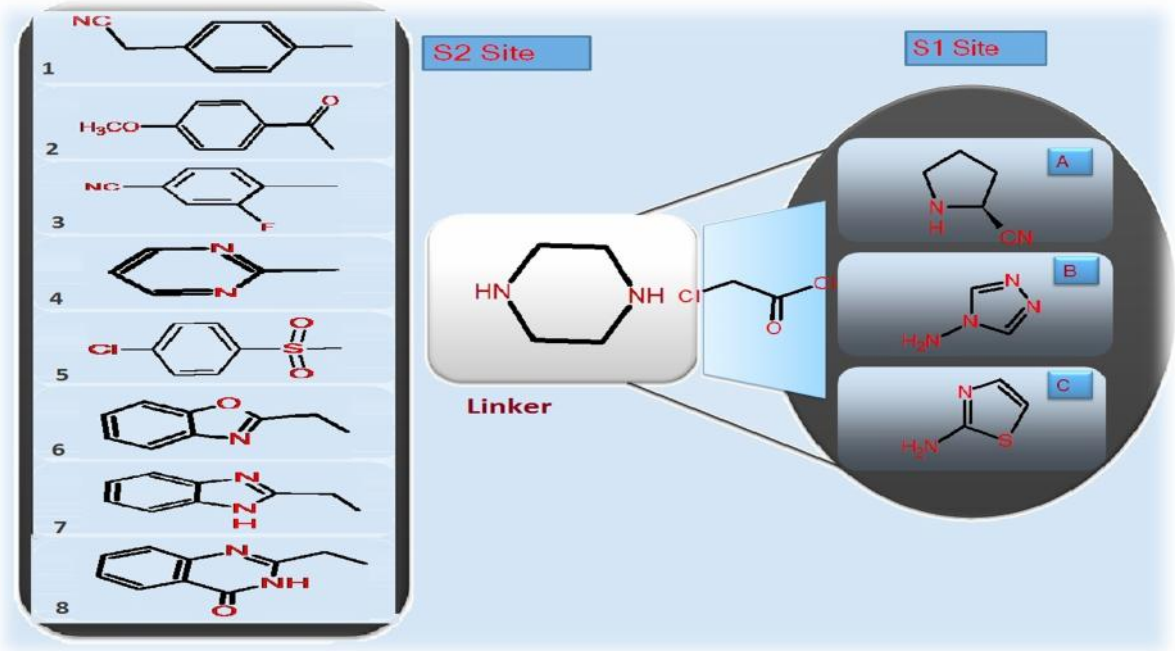

Figure 4.5 Selected fragment in designed molecule at S1 and S2 site

4.2Experimental work

4.2.1 Chemistry

The synthesis of 2(*S*)-cyanopyrrolidine based 1,4-piperazine derivatives is illustrated in Scheme 4.1. Because of its key role in DPP-4 inhibition the 2(*S*)-cyanopyrrolidine moiety has been found to be an integral part of many DPP-4 inhibitors. Thus L-proline was *N*-acylated with chloroacetyl chloride in refluxing THF to afford 1-(2-chloroacetyl) pyrrolidine-2-carboxylic acid. Next, to convert the carboxylic acid moiety to the amide it was treated with dicyclohexylcarbodiimide (DCC) at ambient temperature in dichloromethane followed by ammonium bicarbonate. To prepare the target cyanopyrrolidine a solution of amide in THF was treated with trifluoroacetic anhydride. After completion of the reaction the side product trifluoroacetic acid was neutralized by ammonium bicarbonate and the desired product **4** was isolated [5].

The compound **4** were further subjected to SN_2displacement with 1,4-piperazine to afford the amines **5**[6]. The first series of target compounds **6a-h** were obtained by couplingthe amines **5** with different aromatic and hetroaromatic ring **(a-h)**[7].

In another scheme 2, triazole **(7)** and thiazole **(11)** were reacted with cloroacetyl chloride to obtain compound **8** and compound **12** which were further subjected to SN_2displacement with 1,4-piperazine to afford the amines **9** and **13**. The second **10a-h**and third series **14a-h** of target compounds were obtained by coupling the amines **9** and 13 with different aromatic and hetroaromatic ring **(a-h)**.

2-chloromethyl benzimidazole **(f)** was prepared from condensation of the diamine with chloroacetic acid in the presence of 5 N hydrochloric acid[8]. 2-chloromethyl benzoxazole**(g)** was prepared from condensation of the 2-aminophenol with chloroacetic acid in the presence of glacial acetic acid [9]. The highly accelerated Niementowski synthesis of 2 cholo methyl quinazolin-4(3*H*)-one **(h)** was done by Acid-catalyzed coupling of anthranilic acid with 2 chloroacetamide under microwave irradiation [10].

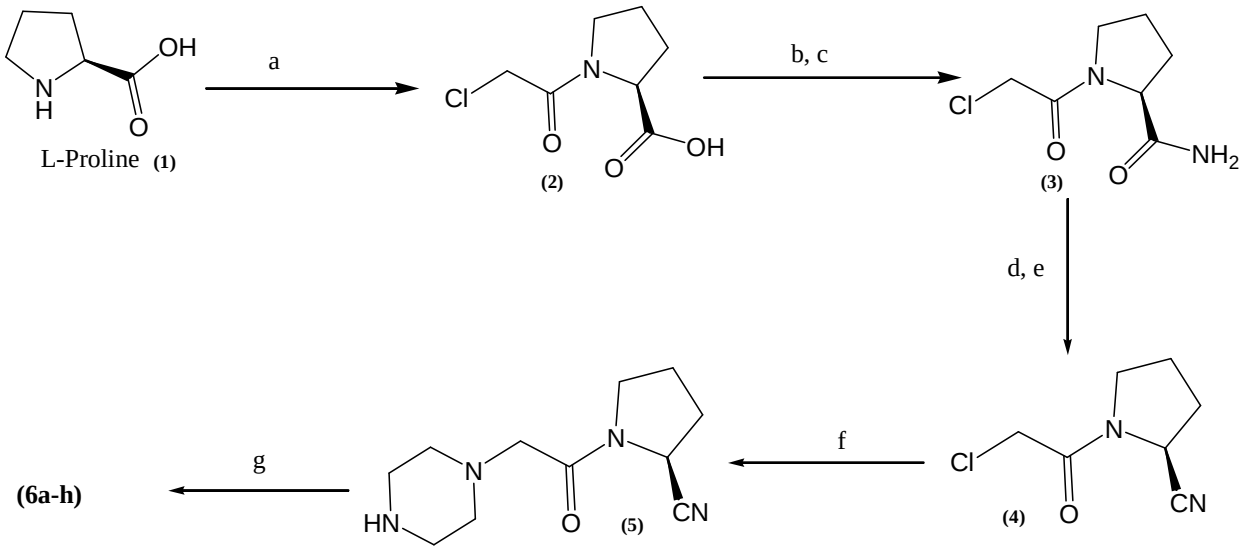

L-Proline **(1)** **(2)** **(3)** **(4)** **(5)**

Scheme 4.1 Reagents and conditions: (a)$ClCH_2COCl$, THF, Reflux (b)DCC, DCM, 15 C, 1h (c)NH_4HCO_3, rt., 1h (d)TFAA, THF, 0 C-RT,1h (e) NH_4HCO_3, 5 C-RT, toluene (f) Piperazine,0 C-RT, 4h, Methanol (g) AcCN, Et_3N, Reflux

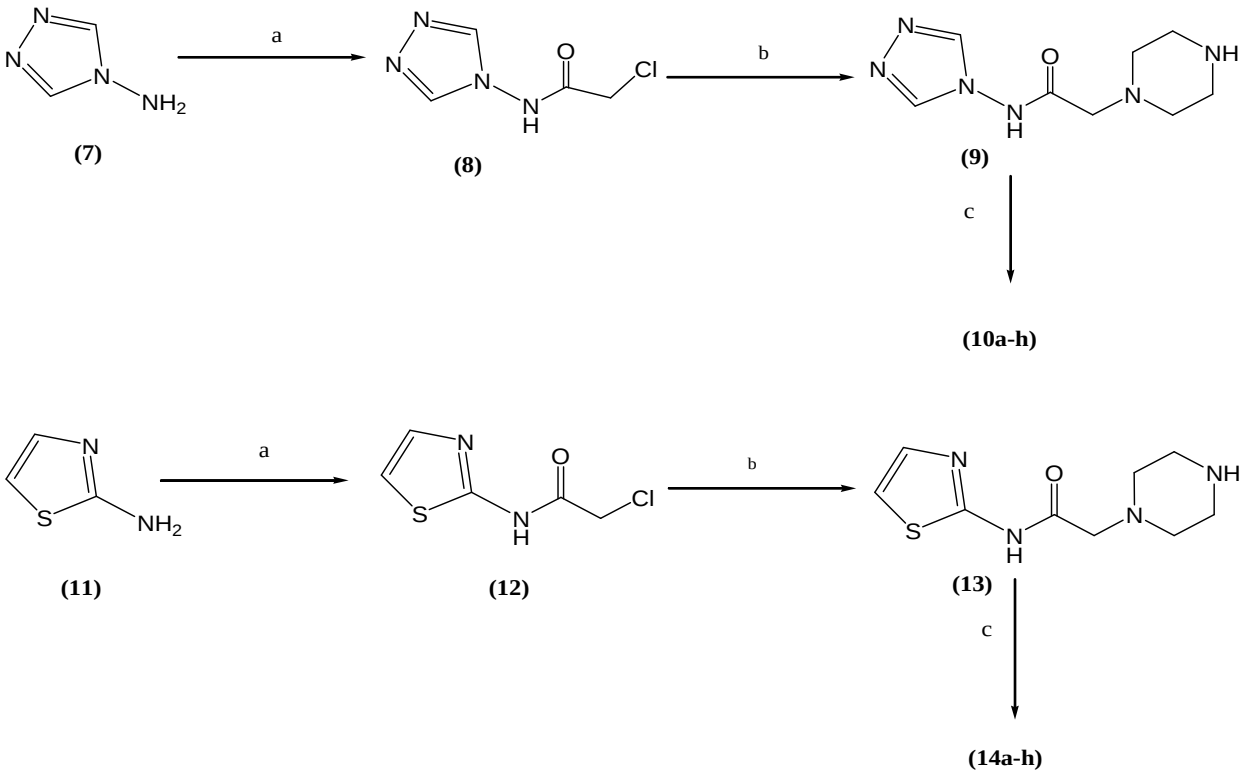

(7) **(8)** **(9)**

Scheme 4.2 Reagents and conditions: (a)$ClCH_2COCl$, DCM, Starring (b) Piperazine,0 C-RT, 4h, Methanol(g)AcCN, Et_3N, Reflux

4.2.2 Synthetic methods and spectroscopic details

All commercially available chemicals were of reagent grade and used as purchased unless stated otherwise. All reactions were performed under an inert atmosphere of dry nitrogen using distilled dry solvents. The melting points of synthesized compounds were determined by open capillary method and were uncorrected. Thin-layer chromatography (TLC) was performed on E. Merck Silica Gel 60-F 254 plates and visualized in UV light (254 nm). The yields were calculated by the last step reaction. Column chromatography was carried out to purify compounds on silica gel [Merck silica gel 60(0.063–0.200 mm)].

The following abbreviations for solvents and reagents are used; tetrahydrofuran (THF), diethyl ether(Et_2O), diisopropyl ether (iPr_2O), toluene($C_6H_5CH_3$), dimethylsulfoxide (DMSO), ethyl acetate(EtOAc), dimethylformamide (DMF), dichloromethane(CH_2Cl_2), chloroform ($CHCl_3$), methanol (MeOH), ethanol(EtOH), acetic acid (AcOH), and hydrochloric acid(HCl).
Infrared spectra were measured using a diffused reflectance JASCO-FTIR spectrometer. The spectra were recorded with a resolution of 4 cm^{-1}, 16 scan were collected for each spectrum and photo radiation were recorded in the range of 400-4000 cm-1. Proton nuclear magnetic resonanceSpectra1H NMR spectra were recorded on a Bruker Avance (400 MHz)spectrometer using deuterated chloroform($CDCl_3$) as solvent at 25°C with tetramethylsilane as the internal standard.. The chemical shift values are reported in parts per million (δ ppm) and coupling constants (J) in hertz (Hz). 13C NMR spectra were also recorded on the Bruker Avance spectrometer. Mass spectra were recorded on an electro-spray ionization mass spectrometer as the value m/z. HPLC purity was determined with an Alliance Waters instrument (model 2695) equipped with a Hypersil BDS C18 column, 250× 4.6 mm, 5 μm and a 2996 UV detector [buffer: 1000 mL water of pH 3.0 with TFA, mobile phase A, buffer : acetonitrile (95:5), mobile phase B, buffer : acetonitrile (10:90), 55 min,220 nm, 1.0 mL/min].Elemental analyses were realized on a CHN rapid elemental analyzer for C, H and N, and the results were within ±0.4 % of the theoretical values.

4.2.2.1 (S) 1-(2-Chloroacetyl)pyrrolidine-2-carboxylic acid (2): To a suspension of L-proline (17.4 mmol) in THF (20 mL) was added chloroacetyl chloride (26.1 mmol) at room temperature and the reaction mixture was refluxed for 2 h. After completion of the reaction, the mixture was cooled to room temperature, diluted with water (20 mL) and stirred for 20 min. The aqueous

layer was re-extracted with ethyl acetate (2 × 50 mL). The combined organic extracts were dried over anhydrous Na_2SO_4 and concentrated under vacuum. The semisolid residue was precipitated in diisopropyl ether. The crystalline white solid was filtered, washed with cold diisopropylether and dried at 40 ° C under vacuum to afford compound 8**.** Mol. Wt. 191.16; M. P: 109-110ºC; Yield: 81%; IR(KBr, cm^{-1}):3470, 3050, 2968, 1743, 1612, 1476, 1349, 787.

4.2.2.2 (S) 1-(2- chloroacetyl)pyrrolidine-2-carboxamide (3): To a solution of compound 8 (5.2 mmol) in dichloromethane (20 mL) was added slowly a solution of dicyclohexylcarbodiimide (5.2 mol) in dichloromethane at 10‑15 ºC (duration 5.0 min) and the mixture was stirred at room temperature for 1 h. To this was added ammonium bicarbonate (0.0522 mol) at precipitated and the mixture was stirred for 1 h. The reaction was monitored by TLC (5% MeOH-$CHCl_3$). After completion of the reaction, the mixture was filtered and the residue was washed with DCM. The filtrates were collected, combined and concentrated under vacuum. The resulting gummy mass was suspended in THF (30 mL) under stirring and diisopropyl ether (20 mL) was slowly added drop wise over 15 min. The mixture was then cooled to 0 ºC and allowed to stand at this temperature for 1 h. The resulting crystalline white solid was filtered, washed with diisopropyl ether and dried under vacuum at 40 ºC to afford the crude product 9 (63.6%). This was then purified by column chromatography (eluting solvent: 2% MeOH/$CHCl_3$) followed by crystallization with diisopropyl ether to afford the pure crystalline compound 9**.** Mol. wt.190.62; M. P: 132-134 ºC; Yield: 45%. IR (KBr, cm^{-1}): 3325, 3037, 2928, 2852, 1730, 1640, 1576, 1088, 648

4.2..2.3 (S) 1-(2-chloroacetyl)pyrrolidine-2-carbonitrile (4): To a suspension of amide 9 (20.9 mmol) in THF (40 mL)was added trifluoroacetic anhydride (4.4 mL, 31.5 mmol) at0‑5 ºC and the reaction mixture was then stirred at room temperature for 2 h. The reaction was monitored by TLC (5%MeOH/$CHCl_3$). To this mixture was added portion wise (over 5 min) ammonium bicarbonate (0.1573 mol) maintaining the temperature of the mixture at 5‑10 ºC. The mixture was stirred at room temperature for 45 min and then concentrated under vacuum at 40 ºC. The residue was stirred in toluene (60 mL) at room temperature for 1.0 h. After filtration, the filtrate was concentrated under vacuum at 40 ºC to afford an oily mass which was stirred in hexane (20 mL) at room temperature for 30 min. The mixture was cooled to 0‑5 ºC and allowed to stand at the same temperature for 30 min. The resulting crystalline solid was filtered and washed with

cold hexane to give the target compound 6. Mol. wt. 172.61; M. P: 52-54ºC. Yield: 80%. IR (KBr, cm^{-1}):3356, 3068, 3005, 2890, 2257, 1634, 1431, 1004, 898, 667

4.2..2.4 (2S)-1-(piperazin-1-ylacetyl)pyrrolidine-2-carbonitrile (5): To the solution of piperazine (11.6 mmol) in methanol (10 ml), the corresponding 1-(2-chloroacetyl)pyrrolidine-2-carbonitrile (5.8mmol) was added drop wise and the reaction was allowed to proceed for 4-6 h at room temperature. To the contents of the reaction mixture, 100 ml of distilled water was then added and the precipitated disubstituted by-products were filtered out. Removal of the solvent under vacuum afforded the crude product which was recrystallized from methanol to obtain crystals of the pure compounds. Mol. wt. 222.28; M. P: 77-78 ºC; Yield: 66% IR(KBr, cm^{-1}): 3482, 3037, 2928, 2852, 2234, 1726, 1551, 1436, 1316

4.2.2.5 (2S)-1-({4-[4-(cyanomethyl)phenyl]piperazin-1-yl}acetyl)pyrrolidine-2-carbonitrile

(6a) General procedure: To a solution of (2*S*)-1-(piperazin-1-ylacetyl)pyrrolidine-2-carbonitrile (4.5 mmol) obtained above in acetonitile was added triethylamine (5.8 mmol) and respective aromatic and hetroaromatic substitution shown in Fig. 5 (4.5 mmol). The reaction mixture was refluxed for 24 h. After reaction, the mixture was diluted with H_2O and then extracted with EtOAc three times. The combined organic layer was dried over $MgSO_4$. The crude product was purified by column chromatography (SiO2, Hexane/EtOAc/CH_2Cl_2 = 1:1:1) to afford the desired compound 6a-6h as powders. Mol. Wt.: 337.42; M. P: 122-124ºC; Yield: 68%; IR (KBr, cm^{-1}): 3170, 2973, 2254, 1785, 1664, 1585, 1495; 1H NMR (CDCl3, δ, J): 7.04 (d, 2H, Ar-H, J=8.0 Hz), 6.73 (d, 2H, Ar-H, J=8.0 Hz), 4.59 (t, 1H, CH-CN, J=12.0 Hz), 3.95 (s, 2H, CH_2-CN), 3.47 (s, 2H, CH_2-CO), 3.46 (t, 2H, Pyrrolidine CH_2, J=12.0 Hz), 3.38 (t, 4H, CH_2 Piperazine, J=8.0 Hz), 2.77 (t, 4H, CH_2 Piperazine, J=8.0 Hz), 2.40 (m, 2H, Pyrrolidine CH_2), 2.01 (t, 2H, Pyrrolidine –CH_2, J=12.0 Hz); 13C NMR ($CDCl_3$, δ ppm):172.12, 149.61, 125.37, 115.55, 60.60, 48.82, 46.68, 31.83, 24.84; ESI-MS: 338.4 (M+1); HPLC purity: 95.5%, Anal. Calcd. For $C_{19}H_{23}N_5O$: C, 67.63; H, 6.87; N, 20.76. Found: C, 68.02; H, 7.17; N, 20.28.

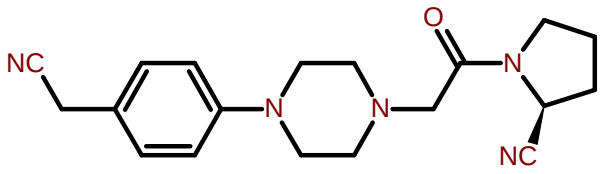

IR

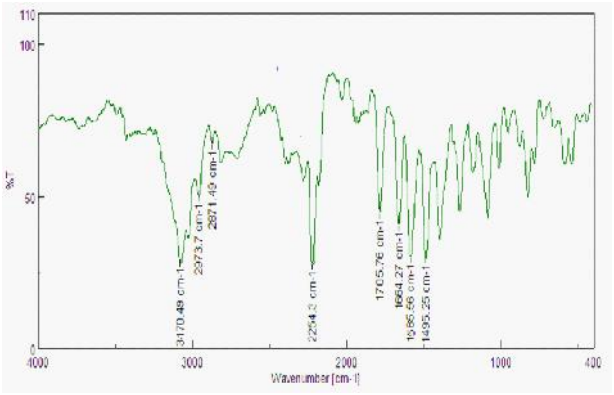

HNMR

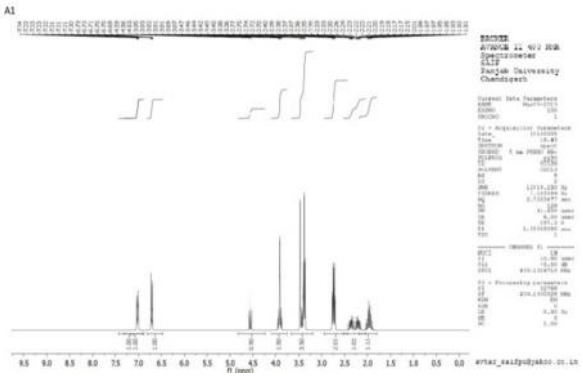

Mass

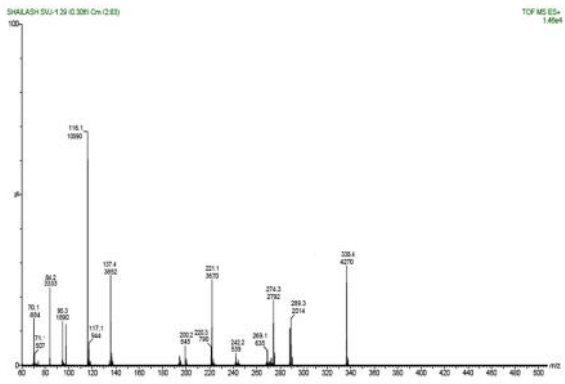

HPLC

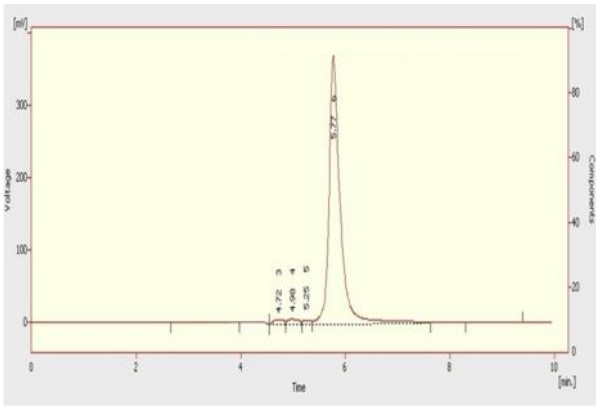

4.2.2.6 (2S)-1-{[4-(4-methoxybenzoyl)piperazin-1-yl]acetyl}pyrrolidine-2-carbonitrile (6b) Mol. Wt.: 356.42; M. P: 132-133 ºC; Yield: 62%; IR (KBr, cm^{-1}): 3086, 3005, 2890, 2257, 1705, 1636, 1431, 1204; 1H NMR ($CDCl_3$, δ, J): 7.63 (d, 2H, Ar-H, J=8.0 Hz), 7.04 (d, 2H, Ar-H, J=8.0 Hz), 4.67 (t, 1H, CH-CN, J=12.0 Hz), 3.92 (t, 2H, CH_2-CO), 3.59 (s, 3H,OCH_3) , 3.46 (s, 2H, Pyrrolidine CH_2, J=12.0 Hz), 2.91 (t, 4H, CH_2 piperazine, J=8.0 Hz), 2.43 (t, 4H, CH_2 piperazine, J=8.0 Hz), 2.24 (m, 2H, CH_2), 2.04 (m, 2H, Pyrrolidine CH_2); 13C NMR ($CDCl_3$) δ ppm: 172.12, 162.71, 131.27, 117.84, 113.17,60.60, 52.15, 48.90, 31.83; ESI-MS: 357.4 (M+1); HPLC purity: 95.3%, Anal. Calcd. For $C_{19}H_{24}N_4O_3$: C, 64.03; H, 6.79; N, 15.72. Found: C, 64.48; H, 6.31; N, 15.29.

***4.2.2.7 (2S)-1-{[4-(4-cyano-2-fluorophenyl)piperazin-1-yl]acetyl}pyrrolidine-2-carbonitrile* (6c)** Mol. Wt.: 341.38; M. P: 133-134 ºC; Yield: 56%; IR (KBr, cm^{-1}): 3124, 2935.16, 2800, 2259, 1765, 1688, 1444, 667; 1H NMR ($CDCl_3$, δ):7.50 (d, 1H,Ar-H, J=8.0 Hz), 7.34 (d, 1H, Ar-H, J=8.0 Hz), 6.96(d, 1H, Ar-H, J=8.0 Hz), 4.73 (t, 1H, Pyrrolidine –CH-CN, J=12.0 Hz) 3.92 (t, 2H, Pyrrolidine CH_2, J=12.0 Hz), 3.63 (t, 4H, CH_2 Piperazine, J=8.0 Hz), 3.55 (s, 2H, CH2-CO), 2.74(t, 4H-CH_2 Piperazine, J=8.0 Hz), 2.41 (m, 2H, Pyrrolidine CH_2, J=12.0 Hz), 2.03 (m, 2H, Pyrrolidine –CH_2); 13C NMR ($CDCl_3$, δ ppm): 172.12, 152.34, 133.31, 126.37, 117.84, 111.48, 60.60, 52.70, 46.48, 31.83; ESI-MS: 342.3 (M+1); HPLC purity: 95.8%, Anal. Calcd. For $C_{18}H_{20}FN_5O$: C, 63.33; H, 5.91; F, 5.57; N, 20.51. Found: C, 62.96; H, 5.57; N, 20.77.

4.2.2.8 (2S)-1-{[4-(pyrimidin-2-yl)piperazin-1-yl]acetyl}pyrrolidine-2-carbonitrile (6d) Mol. Wt.: 300.36; M. P: 120-122 ºC; Yield: 62%; IR (KBr, cm^{-1}):3178, 2900, 2270, 1752, 1617, 1400, 1100; 1H NMR ($CDCl_3$, δ, J): 8.37 (d, 2H, Ar-H, J=8.0 Hz), 6.54 (t, 1H, Ar-H, J=8.0 Hz), 4.89 (t, 1H Pyrrolidine–CH-CN, J=12.0 Hz), 3.95(s, 2H, Pyrrolidine –CH_2), 3.47 (s, 2H, CH_2-CO), 3.46 (t, 2H, -CH_2 Piperazine, J=8.0 Hz), 2.72 (t, 2H, -CH2 Piperazine, J=8.0 Hz), 2.42 (m, 2H, 17 Pyrrolidine –CH_2), 2.16 (m, 2H, Pyrrolidine –CH_2); 13C NMR ($CDCl_3$, δ ppm): 172.12, 160.59, 158.04, 117.84, 110.35, 60.60, 52.70, 46.68, 31.83; ESI-MS: 301.4 (M+1); HPLC purity: 96.3%, Anal. Calcd. For $C_{15}H_{20}N_6O$: C, 59.98; H, 6.71; N, 27.98. Found: C, 59.35; H, 7.14; N, 27.43.

4.2.2.9 (2S)-1-({4-[(4-chlorophenyl)sulfonyl]piperazin-1-yl}acetyl)pyrrolidine-2-carbonitrile (6e) Mol. Wt.: 396.89; M. P: 138-138ºC; Yield: 59.5%; IR (KBr, cm^{-1}): 3001, 2978, 2118, 1794,1582, 1304, 782; 1H NMR ($CDCl_3$, δ, J): 7.76 (d, 2H, Ar-H, J=8.0 Hz), 7.63 (d, 2H, Ar-H, J=8.0 Hz), 4.59 (t, 1H, Pyrrolidine –CH-CN, J=12.0 Hz), 3.68 (m, 2H, Pyrrolidine –CH_2), 3.25 (s, 2H, CH_2-CO), 3.13 (t, 2H, -CH_2 Piperazine, J=8.0 Hz), 2.72 (t, 2H, -CH_2 Piperazine, J=8.0 Hz), 2.47 (m, 2H, Pyrrolidine –CH_2), 2.23 (m, 2H, Pyrrolidine –CH_2); 13C NMR ($CDCl_3$, δ ppm): 172.12, 139.95, 129.72, 117.84, 60.60, 52.94,48.90, 31.83, 23.99; ESI-MS: 397.2(M+1), 398.2(M+2); HPLC purity: 95.4%, Anal. Calcd. For $C_{17}H_{21}ClN_4O_3S$: C, 51.45; H, 5.33; Cl, 8.93; N, 14.12. Found: 51.86; H, 5.76; Cl, 8.23; N, 14.63.

4.2.2.10 (2S)-1-{[4-(1,3-benzoxazol-2-ylmethyl)piperazin-1-yl]acetyl}pyrrolidine-2carbonitrile (6f) Mol. Wt.: 353.42; M. P: 136-137ºC; Yield: 62%; IR (KBr, cm^{-1}): 3131, 2973, 2870, 2231,1669, 1592, 1240; 1H NMR ($CDCl_3$, δ, J):7.69 (m, 4H, Ar-H), 4.76 (t, 1H, Pyrrolidine –CH-CN, J=12.0 Hz), 3.93 (m, 2H, Pyrrolidine CH_2), 3.52 (s, 2H, CH_2), 3.25 (s, 2H , CH2-CO), 2.76 (t, 4H, -CH_2 Piperazine, J=8.0 Hz), 2.42 (t, 4H, -CH_2 Piperazine, J=8.0 Hz), 2.21 (m, 2H,

Pyrrolidine –CH2), 2.03 (m, 2H, Pyrrolidine –CH_2); 13C NMR ($CDCl_3$, δ ppm): 170.29, 151.20, 140.21, 122.56, 119.88, 112.20, 60.60, 53.58, 48.90; ESI-MS: 354.4 (M+1); HPLC purity: 96.2%, Anal. Calcd. For $C_{19}H_{23}N_5O_2$: C, 64.57; H, 6.56; N, 19.82. Found: C, 64.86; H, 6.93; N, 20.03.

4.2.2.11 (2S)-1-{[4-(1H-benzimidazol- 2-ylmethyl) piperazin-1-yl]acetyl} pyrrolidine -2 carbonitrile (6g) Mol. Wt.: 352.43; M. P: 133-135 ºC; Yield: 61%; IR (KBr, cm^{-1}): 3339, 3100, 2976, 2236, 1720, 1590, 1477, 1015; 1H NMR ($CDCl_3$, δ, J): 7.55 (d, 2H, Ar-H, J=8.0 Hz), 7.18 (d, 2H, Ar-H, J=8.0 Hz), 4.87 (t, 1H-NH, J=8.0 Hz), 4.21 (s, 2H, -CH_2), 3.81 (m, 1H, Pyrrolidine –CH-CN), 3.53 (s, 2H, Pyrrolidine –CH_2), 2.94 (s, 2H, CH_2-CO), 2.74 (t, 4H, CH_2 Piperazine, J=8.0 Hz), 2.47 (t, 4H, CH2 Piperazine, J=8.0 Hz), 2.15 (m, 2H, Pyrrolidine –CH_2); 13C NMR ($CDCl_3$, δ ppm): 169.70, 145.73, 138.87, 121.85, 115.56, 62.42, 54.43, 48.53, 31.01; ESI-MS: 353.4 (M+1); HPLC purity: 95.3%, Anal. Calcd. For $C_{19}H_{24}N_6O$: C, 64.75; H, 6.86; N, 23.85. Found: C, 64.34; H, 6.38; N, 24.05.

4.2.2.12 (2S)-1-{4-[4-oxo-3,4-dihydroquinazolin-2-yl)methyl)piperazin 1yl]acetyl}pyrrolidine-2-carbonitrile (6h) Mol. Wt.: 380.44; M. P: 141-143ºC; Yield: 58%, IR (KBr, cm^{-1}): 3386, 3092, 3041, 2225, 1786, 1590, 1100; 1H NMR ($CDCl_3$, δ, J): 8.08 (t, 1H-NH), 7.78 (d, 1H, Ar-H, J=8.0 Hz), 7.64 (d, 1HAr-H, J=8.0 Hz), 7.49 (d, 1H, Ar-H, J=8.0 Hz), 4.49 (t, 1H, Pyrrolidine –CHCN, J=12.0 Hz), 3.64 (m, 1H, Pyrrolidine –CH_2), 3.35 (s) (2H, CH_2-CO), 3.25 (s, 2H, CH_2), 2.46 (t, 4H, -CH_2 Piperazine, J=8.0 Hz), 13C NMR ($CDCl_3$, δ ppm): 172.12, 162.84, 151.54, 147.15, 130.12,126.03, 121.66, 117.84, 58.19; ESI-MS: 381.1 (M+1); HPLC purity: 95.5%, Anal. Calcd. For $C_{20}H_{24}N_6O_2$: C, 63.14; H, 6.36; N, 22.09. Found: C, 62.95; H, 6.07; N, 21.89.

4.2.2.13 2-chloro-N-(4H-1,2,4-triazol-4-yl)acetamide (8) Chloroacetyl chloride (11.9 mmol) was added dropwise to a solution of 4-amino 1,2,4 triazole (11.9 mmol) in DCM (100 mL) at 0ºC. Then the mixture was stirred at room temperature for 12 h. The resulting mixture was quenched by addition of water and extracted with dichloromethane. The combined organic layer was dried over anhydrous MgSO4, filtered, and concentrated under reduced pressure. The residue was purified by recrystallization (EtOAc and hexane) to give product. Mol. Wt.: 160.56; M. P: 88-89 ºC; Yield: 72%; IR (KBr, cm^{-1}):3332, 3010, 2916, 1726, 1636, 1551, 1316, 816.

4.2.2.14 2-(piperazin-1-yl)-N-(4H-1,2,4-triazol-4-yl)acetamide (9) To the solution of piperazine (12.4 mmol) in methanol (10 ml), the corresponding 2-chloro-*N*-(4*H*-1,2,4-triazol-4-yl) acetamide (6.2 mmol) were added drop wise and the reaction was allowed to proceed for 4-6 h at

room temperature. To the contents of the reaction mixture, 100 ml of distilled water was then added and the precipitated disubstituted by-products were filtered out. Removal of the solvent under vacuum afforded the crude product which was recrystallized from methanol to obtain crystals of the pure compounds. Mol. Wt.:210.23; M. P: 94-96ºC; Yield: 70%; IR (KBr, cm^{-1}):3339, 3004, 2972, 1726, 1656, 1436, 1316.

4.2.2.15 2-{4-[4-(cyanomethyl)phenyl]piperazin-1-yl}-N-(4H-1,2,4-triazol-4-yl)acetamide (10a)

General procedure To a solution of 2-(piperazin-1-yl)-*N*-(4*H*-1,2,4-triazol-4-yl)acetamide (4.7 mmol) obtained above in acetonitile was added triethylamine (5.8 mmol) and respective aromatic and hetroaromatic substitution shown in Fig. 5 (4.7 mmol). The reaction mixture was refluxed for 24 h. After reaction, the mixture was diluted with H_2O and then extracted with EtOAc three times. The combined organic layer was dried over $MgSO_4$. The crude product was purified by column chromatography (SiO_2, Hexane/EtOAc/CH_2Cl_2 = 1:1:1) to afford the desired compound 10a-10h as powders in 50–79% yield. Mol. Wt.: 325.37; M. P: 110-111ºC; Yield: 65%; IR(KBr, cm^{-1}):3410, 3004, 2972, 2224, 1788,1664, 1589, 1498; 1HNMR ($CDCl_3$, δ, J): 8.50 (s, 1H-CH-N), 8.45 (s, 1H-NH), 7.04 (d, 2H, Ar-H), 6.70 (d, 2H,Ar-H), 3.92 (s, 2H, CH_2-CN), 3.58 (s, 2H-CH_2-CO), 3.40 (t, 4H-CH_2Piperazine), 2.74 (t, 4H, CH_2 Piperazine); 13C NMR ($CDCl_3$,δ ppm):165.08, 150.98, 149.61, 141.51, 127.71, 115.55, 57.23, 52.70, 24.84; ESI-MS: 326.1 (M+1); HPLC purity: 96.9%, Anal. Calcd. For$C_{16}H_{19}N_7O$: C, 59.06; H, 5.89; N, 30.13. Found: C, 58.89; H, 6.08; N, 29.89.

4.2.2.16 2-[4-(4-methoxybenzoyl)piperazin-1-yl]-N-(4H-1,2,4-triazol-4-yl)acetamide(10b) Mol. Wt.: 344.37 M. P: 114-115ºC; Yield: 62%; IR(KBr, cm^{-1}):3495, 3037, 2928, 2852, 1740, 1688, 1540, 1413, 1182; 1HNMR ($CDCl_3$, δ, J):8.50 (s) (1H, -NH), 8.53 (s, 2H, -CH-N), 7.58 (d, 2H, Ar-H), 7.04 (d, 2H, Ar-H), 3.80 (s, 2H, -OCH_3, 3.71 (s, 2H, -CH2-CO), 3.69 (t, 4H, CH_2Piperazine), 2.87 (t, 4H, CH_2Piperazine); 13C NMR ($CDCl_3$, δ ppm):170.64, 162.71, 150.98, 141.51, 131.27, 113.17, 57.23, 45.38; ESI-MS: 344.3 (M+1); HPLC purity: 96.3%, Anal. Calcd. For$C_{16}H_{20}N_6O_3$: C, 55.80; H, 5.85; N, 24.40. Found: C, 55.36; H, 5.55; N, 24.20.

4.2.2.17 2-[4-(4-cyano-2-fluorophenyl)piperazin-1-yl]-N-(4H-1,2,4-triazol-4-yl)acetamide(10c) Mol. Wt.: 329.33 M. P: 116-118 ºC; Yield: 60%; IR (KBr, cm^{-1}):3441, 3020, 2977, 2120, 1719, 1689, 1590, 610; 1HNMR ($CDCl_3$, δ, J): 8.88 (s, 1H NH), 8.44(s, 1H CH-N), 8.17(s, 1H CH-N), 7.50 (s, 1H, Ar-H), 7.34 (d, 1HAr-H), 6.91(d, 1HAr-H), 3.67 (t, 4H, Ar H), 3.53 (s, 2H, CH_2-CO) , 2.74 (t, 4H, CH_2Piperazine); 13C NMR ($CDCl_3$,δ ppm):165.08, 152.34, 141.51, 133.31,

122.49, 116.71,111.48, 57.23; ESI-MS: 330.1 (M+1); HPLC purity: 96.5%, Anal. Calcd. For$C_{15}H_{16}FN_7O$: C, 54.70; H, 4.90; N, 29.77. Found: C, 55.11; H, 4.49; N, 29.25.

4.2.2.18 2-[4-(pyrimidin-2-yl)piperazin-1-yl]-N-(4H-1,2,4-triazol-4-yl)acetamide (10d) Mol. Wt.: 288.31 M. P: 108-110ºC; Yield: 62%; IR(KBr, cm^{-1}):3578, 3034, 1779, 1617, 1500, 1445; 1HNMR ($CDCl_3$, δ, J): 8.43 (s, 1H) CH of pyridine ring (meta), 8.37 (s, 2H, CH-N), 8.18 (s, 1H, -NH) , 6.54 (s, 1H, CH of pyridine ring (p)), 3.82 (t, 4H, CH_2Piperazine) , 3.50 (s, 2H-CH_2-CO), 2.85 (t, 4H, CH_2Piperazine) 13C NMR ($CDCl_3$,δ ppm):165.08, 160.59, 150.98, 141.15, 110.36, 57.23, 52.70, 46.45; ESI-MS: 289.3 (M+1); HPLC purity: 95.3%, Anal. Calcd. For$C_{12}H_{16}N_8O$: C, 49.99; H, 5.59; N, 38.87. Found: C, 49.46; H, 5.32; N, 38.36.

4.2.2.19 2-{4-[(4-chlorophenyl)sulfonyl]piperazin-1-yl}-N-(4H-1,2,4-triazol-4- yl)acetamide (10e) Mol. Wt.: 384.84; M. P:118-120ºC; Yield: 65%; IR (KBr, cm^{-1}): 3431, 3008, 2896, 1728, 1638, 1525, 1345, 650; 1H NMR ($CDCl_3$, δ, J): 8.84 (s, 2H-CH-N), 8.43 (s, 1H, NH), 7.80 (d, 1H, Ar-H), 7.63 (d,1H, Ar-H), 3.59(s,2H, CH_2-CO), 3.11 (t, 4H-CH_2Piperazine), 2.84 (t, 4H-CH_2Piperazine); 13C NMR ($CDCl_3$, δ ppm): 165.08, 150.98, 141.51, 138.92, 129.57, 57.23, 52.94, 46.05; ESI-MS: 385.4 (M+1), 386.4 (M+2); HPLC purity: 96.2%, Anal. Calcd. For $C_{14}H_{17}ClN_6O_3S$: C, 43.69; H, 4.45; N, 21.84. Found: C, 43.69; H, 4.09; Cl, 9.29; N, 21.25.

4.2.2.20 2-[4-(1,3-benzoxazol-2-ylmethyl)piperazin-1-yl]-N-(4H-1,2,4-triazol-4-yl)acetamide (10f) Mol. Wt.: 288.31M. P: 122-123ºC; Yield: 68%; IR(KBr, cm^{-1}):3341, 3041, 2919, 1746, 1630, 1516, 1065; 1HNMR ($CDCl_3$, δ, J): 8.43(s, 2H, CH-N), 8.17 (s, 1H, NH), 7.64 (d, 2H, Ar-H), 6.70 (d, 2H, Ar-H), 3.92 (s, 2H-CH_2), 3.48 (s, 2H,CH_2-CO), 2.69 (t, 4H, Ar-H), 2.43 (t, 4H, Ar-H) 13C NMR ($CDCl_3$,δ ppm):170.29, 165.08, 150.98, 122.56, 119.88, 112.20, 57.23, 52.73; ESI-MS: 342.2 (M+1); HPLC purity: 96.7%, Anal. Calcd. For $C_{12}H_{16}N_8O$: C, 49.99; H, 5.59; N, 38.87. Found: C, 49.28; H, 5.21; N, 38.43.

4.2.2.21 2-[4-(1H-benzimidazol-2-ylmethyl)piperazin-1-yl]-N-(4H-1,2,4-triazol-4- yl)acetamide (10g) Mol. Wt.: 340.38; M. P: 124-126ºC; Yield: 67%; IR(KBr, cm^{-1}):3443, 3005, 2843, 1741, 1686, 1591, 1431, 1034; 1HNMR ($CDCl_3$, δ, J): 8.88 (s, 1H, CH-N), 8.17 (s, 1H, NH), 7.55 (d), Ar-H), 7.18 (d, Ar-H), 4.26 (s, CH_2), 3.55 (s), CH_2-CO), 2.90 (t, 4H, CH_2Piperazine), 2.59 (t, 4H, CH_2Piperazine); 13C NMR ($CDCl_3$,δ ppm):165.08, 150.98, 144.97, 141.64, 124.78,117.82, 112.48, 54.43; ESI-MS: 341.3 (M+1); HPLC purity: 96.8%, Anal. Calcd. For$C_{16}H_{20}N_8O$: C, 56.46; H, 5.92; N, 32.92. Found: C, 56.95; H, 5.42; N, 33.08.

4.2.2.22 2-{4-[(4-oxo-3,4-dihydroquinazolin-2-yl)methyl]piperazin-1-yl}-N-(4H-1,2,4-triazol-4-yl)acetamide (10h) Mol. Wt.: 368.39; M. P: 134-135 ºC; Yield: 69%; IR (KBr, cm^{-1}):3477, 3037, 2898, 1723, 1640, 1578; 1H NMR ($CDCl_3$, δ, J):9.03-8.44(s, 2H, CH-N), 8.22 (s, 1H, NH), 8.44 (d, 1H, Ar-H, J=8.0 Hz), 7.78 (d, 1H, Ar-H, J=8.0 Hz), 7.64(d,1H, Ar-H, J=8.0 Hz), 7.49(d, 1H, Ar-H, J=8.0 Hz), 3.86 (s, 2H, CH_2), 3.49 (s, 2H, -CH_2-CO), 2.64 (t, 2H, CH_2 Piperazine, J=8.0 Hz), 2.45 (t, 2H, CH_2 Piperazine, J=8.0 Hz); 13C NMR ($CDCl_3$, δ ppm): 162.84, 151.54, 147.15, 141.51, 130.12, 126.03, 121.66, 58.19; ESI-MS: 369.4 (M+1); HPLC purity: 95.9%, Anal. Calcd. For $C_{17}H_{20}N_8O_2$: C, 55.43; H, 5.47; N, 30.42. Found: C, 55.14; H, 5.26; N, 30.75.

4.2.2.23 2-chloro-N-(1,3-thiazol-2-yl)acetamide (12) Chloroacetyl chloride (10 mmol) was added dropwise to a solution 2-amino thiazole (10 mmol) in DCM (100 mL) at 0ºC. Then the mixture was stirred at room temperature for 10 h. The resulting mixture was quenched by addition of water and extracted with dichloromethane. The combined organic layer was dried over anhydrous MgSO4, filtered, and concentrated under reduced pressure. The residue was purified by recrystallization (EtOAc and hexane) to give product. Mol. Wt.: M. P: 89-90ºC; Yield: 75%; IR (KBr, cm^{-1}):3410, 3004, 2972, 1707, 1600, 1400, 7

***4.2.2.24* 2-(piperazin-1-yl)-*N*-(1,3-thiazol-2-yl)acetamide (13)** To the solution of piperazine (11.3 mmol) in methanol (10 ml), the corresponding 2-chloro-N-(1,3-thiazol-2-yl)acetamide (5.6 mmol) were added drop wise and the reaction was allowed to proceed for 4-6 h at room temperature. To the contents of the reaction mixture, 100 ml of distilled water was then added and the precipitated disubstituted by-products were filtered out. Removal of the solvent unde vacuum afforded the crude product which was recrystallized from methanol to obtain crystals of the pure compounds. Mol. Wt.: M. P: 94-95ºC; Yield: 74%; IR (KBr, cm^{-1}):3410, 3008, 3017, 2934, 1788, 1600, 1400.

4.2.2.25 2-{4-[4-(cyanomethyl)phenyl]piperazin-1-yl}-N-(1,3-thiazol-2-yl)acetamide (14a)

General procedure: To a solution of 2-(piperazin-1-yl)-*N*-(1,3-thiazol-2-yl)acetamide (4.4 mmol) obtained above in acetonitile was added triethylamine (5.8 mmol) and respective aromatic and hetroaromatic substitution shown in Fig. 5 (4.4 mmol). The reaction mixture was refluxed for 24 h. After reaction, the mixture was diluted with H_2O and then extracted with EtOAc three times. The combined organic layer was dried over $MgSO_4$. The crude product was purified by column chromatography (SiO2, Hexane/EtOAc/CH_2Cl_2 = 1:1:1) to afford the desired compound

14a-14h as powders in 50–79% yield Mol. Wt.: 341.43 M. P: 110-112 ºC; Yield: 68%; IR (KBr, cm^{-1}):3410, 3093, 2967, 2224, 1697, 1670, 1523, 1486, 1316; 1H NMR ($CDCl_3$, δ, J): 7.54 (s, 1H, NH,), 7.52(d, 1H -CH-N, J=8.0 Hz), 7.30(d, 1H, CH-N, J=8.0 Hz), 7.05(d, 2H, Ar-H), 6.72(d, 2H, Ar-H), 3.93(s, 2H, CH_2-CN), 3.40(s, 2H, -CH_2-CO), 3.40(t, 4H, CH_2 Piperazine J=8.0 Hz), 2.74(t, 4H, CH2 Piperazine, J=8.0 Hz); 13C NMR ($CDCl_3$, δ ppm): 171.49, 162.93, 149.61, 137.29, 117.10, 115.55, 110.86, 59.74, 48.82, 24.84; ESI-MS: 342.3 (M+1); HPLC purity: 98.5%, Anal. Calcd. For $C_{17}H_{19}N_5OS$: C, 59.80; H, 5.61; N, 20.51. Found: C, 59.21; H, 5.24; N, 20.34.

4.2.2.26 2-[4-(4-methoxybenzoyl)piperazin-1-yl]-N-(1,3-thiazol-2-yl)acetamide(14b) Mol. Wt.: 360.43 M. P: 115-116 ºC; Yield: 65%; IR (KBr, cm^{-1}):3428, 3171, 3076.8, 2818, 1700, 1693, 1577; 1H NMR ($CDCl_3$, δ, J): 7.67(d, 2H, Ar-H), 7.54 (d, 1H, Ar-H), 7.30 (d, 1H, CH-N thiazole ring), 7.04 (d, 2H, Ar-H, J=8.0 Hz), 3.83 (s, 3H, CH_3O), 3.81 (s, 2H, CH_2-CO), 3.06 (t, 4H-CH_2 Piperazine, J=8.0 Hz),2.63(t, 4H, CH_2 Piperazine, J=8.0 Hz), 13C NMR ($CDCl_3$, δ ppm): 171.39, 162.93, 137.29, 130.94, 113.17, 59.54, 52.77, 45.38, ESI-MS: 361.4 (M+1). HPLC purity: 97.8%, Anal. Calcd. For $C_{17}H_{20}N_4O_3S$: C, 56.65; H, 5.59; N, 15.54. Found: C, 56.34; H, 5.34; N, 15.26.

4.2.2.27 2-[4-(4-cyano-2-fluorophenyl)piperazin-1-yl]-N-(1,3-thiazol-2-yl)acetamide(14c) Mol. Wt.: 345.39 M. P: 117-118ºC; Yield: 62%; IR (KBr, cm^{-1}):3499, 3168, 2260, 1742, 1691, 1582, 742; 1H NMR ($CDCl_3$, δ, J): 7.54 (s, 1H, NH), 7.54 (s, 1H, CH-N thiazole ring), 7.52 (s, 1H, CH-N thiazole ring), 7.48 (s, 1H, Ar-H), 7.32 (d, 1H, Ar-H, J=8.0 Hz), 6.95 (d, 1H, Ar-H, J=8.0 Hz), 3.73 (s, 2H, CH_2-CO), 3.50 (t, 4H, CH_2 Piperazine, J=8.0 Hz), 2.74 (t, 4H, -CH_2 Piperazine, J=8.0 Hz); 13C NMR ($CDCl_3$, δ ppm): 171.39, 162.93, 152.34, 137.29, 132.25, 126.37, 122.49, 116.71, 110.86, 59.74; ESI-MS: 346.3 (M+1), HPLC purity: 98.2%, Anal. Calcd. For $C_{16}H_{16}FN_5OS$: C, 55.64; H, 4.67; F, 5.50; N, 20.28. Found: C, 55.81; H, 4.34; F, 5.18; N, 19.89.

4.2.2.28 2-[4-(pyrimidin-2-yl)piperazin-1-yl]-N-(1,3-thiazol-2-yl)acetamide(14d) Mol. Wt.: 304.37 M. P: 111-112ºC; Yield: 64%; IR (KBr, cm^{-1}):3410, 3167, 2952, 1716, 1697, 1572; 1H NMR ($CDCl_3$, δ, J): 8.37(s, 1H, -NH), 8.37 (s, 1H, CH-N thiazole ring), 8.35 (s, 1H, CH-N thiazole ring), 7.54 (1H, CH of pyridine ring), 7.30 (1H CH of pyridine ring), 6.54 (1H, CH of pyridine ring), 3.80 (t, 4H, CH_2 Piperazine, J=8.0 Hz), 3.34 (s, 2H, CH_2-CO), 2.76 (t, 4H, CH_2 Piperazine, J=8.0 Hz); 13C NMR ($CDCl_3$, δ ppm): 171.39, 160.59, 158.04, 137.29, 110.86,

59.74, 52.70, 46.45; ESI-MS: 305.2 (M+1), HPLC purity: 97.6%, Anal. Calcd. For $C_{13}H_{16}N_6OS$: C, 51.30; H, 5.30; N, 27.61. Found: C, 51.76; H, 5.81; N, 27.23.

4.2.2.29 2-{4-[(4-chlorophenyl)sulfonyl]piperazin-1-yl}-N-(1,3-thiazol-2-yl)acetamide(14e) Mol. Wt.: 400.9 M. P: 122-124ºC; Yield: 62%; IR (KBr, cm^{-1}):3340, 3170, 2919, 2853, 1736, 1696,1515, 1185, 856; 1H NMR (CDCl3, δ, J): 7.81(d, 2H,Ar-H, J=8.0 Hz), 7.63 (d, 2H, Ar-H, J=8.0 Hz), 77.54 (d, 1H, Ar-H, J=8.0 Hz), 7.30 (d, 1H, -CH-N thiazole ring) 3.68 (s, 2H, $-CH_2$-CO), 3.35 (t, 4H,$-CH_2$ Piperazine, J=8.0 Hz), 2.79 (t, 4H, CH_2 Piperazine, J=8.0 Hz); 13C NMR ($CDCl_3$, δ ppm): 171.39, 162.93,139.95, 137.29, 129.72, 110.86, 59.74, 52.94, 46.05; ESI-MS: 401.2 (M+1), 402.2(M+2), HPLC purity: 96.2%, Anal. Calcd. For $C_{15}H_{17}ClN_4O_3S_2$: C, 44.94; H, 4.27; N, 13.98. Found: C, 44.29; H, 4.76; N, 13.19.

4.2.2.30 2-[4-(1,3-benzoxazol-2-ylmethyl)piperazin-1-yl]-N-(1,3-thiazol-2-yl)acetamide(14f) Mol. Wt.: 357.43; M. P: 112-114 ºC; Yield: 64%; IR (KBr, cm^{-1}):3440, 3041, 2900, 2841, 1728, 1695, 1583, 1491; 1H NMR ($CDCl_3$, δ, J): 7.65(d, 2H, Ar-H), 7.60 (d,1H, Ar-H), 7.54 (d,1H, CH-N thiazole ring), 7.30(d, 2H, CH-N thiazole ring), 3.89 (s, 2H, CH_2), 3.38 (s, 2H, $-CH_2$-CO), 2.82 (t, 4H, $-CH_2$ Piperazine, J=8.0 Hz), 2.51(t, 4H $-CH_2$ Piperazine, J=8.0 Hz); 13C NMR ($CDCl_3$, δ ppm): 170.29, 162.93, 151.20, 140.21, 137.29, 125.00, 119.88, 110.86, 59.74, 52.73; ESI-MS: 358.4 (M+1); HPLC purity: 97.4%, Anal. Calcd. For $C_{17}H_{19}N_5O_2S$: C, 57.12; H, 5.36; N, 19.59. Found: C, 57.73; H, 5.85; N, 19.31.

4.2.2.31 2-[4-(1H-benzimidazol-2-ylmethyl)piperazin-1-yl]-N-(1,3-thiazol-2-yl)acetamide (14g) Mol. Wt.: 356.45 M. P: 110-112ºC; Yield: 61%; IR (KBr, cm^{-1}):3360, 3140, 2927, 1726, 1685, 1526; 1H NMR (CDCl3, δ, J): 7.55(d, 2H, Ar-H), 7.49(d, 1H, CH-N thiazole ring), 7.30(d, 1H, CH-N thiazole ring), 7.18 (d, 1H, Ar-H, J=8.0 Hz), 4.30 (s, 2H, $-CH_2$), 3.41(s, 2H, CH_2-CO), 3.00 (t, 4H, CH_2 Piperazine, J=8.0 Hz), 2.61(t, 4H, CH_2 Piperazine, J=8.0 Hz); 13C NMR ($CDCl_3$, δ ppm): 171.28, 162.34, 144.97, 141.64, 138.85, 124.78, 121.17, 117.82, 112.48, 54.43;ESI-MS: 357.1 (M+1); HPLC purity: 96.5%, Anal. Calcd. For $C_{17}H_{20}N_6OS$: C, 57.28; H, 5.66; N, 23.58; S, 9.00. Found: C, 57.51; H, 5.43; N, 23.63.

4.2.2.31 2-{4-[(4-oxo-3,4-dihydroquinazolin-2-yl) methyl]piperazin-1-yl} -N-(1,3-thiazol-2 yl) acetamide (14h) Mol. Wt.: 384.46 M. P: 122-124ºC; Yield: 60%; IR (KBr, cm^{-1}): 3341, 3097, 2882, 1716, 1606, 1590, 1483; 1H NMR ($CDCl_3$, δ, J): 8.08 (d, 1H, Ar-H, J=8.0 Hz), 7.78 (d, 1H, CH-N thiazole ring), 7.64 (d, 1H-CH, Ar-H, J=8.0 Hz), 7.54 (1H, CH-N thiazole ring), 7.49(d, 1H, Ar-H, J=8.0 Hz), 7.30 (d, 1H, Ar-H, J=8.0 Hz), 4.90 (s, 2H, CH_2), 3.40(s, 2H, CH_2-

CO), 2.66 (t, 4H, CH_2 Piperazine, J=8.0 Hz), 2.49 (t, 4H, CH_2 Piperazine, J=8.0 Hz); 13C NMR ($CDCl_3$, δ ppm): 171.43, 162.84, 151.54, 147.15, 130.12, 126.03, 124.30, 110.86, 58.19, 53.85; ESI-MS: 385.3 (M+1); HPLC purity: 96.9%, Anal. Calcd. For $C_{18}H_{20}N_6O_2S$: C, 56.23; H, 5.24; N, 21.86; S, 8.34. Found: C, 56.64; H, 5.74; N, 22.21.

4.3 Result and discussion

4.3.1Acivity and selectivity Prediction

Structure–activity relationship as well as selectivity of the piperazinyl derivatives described above need to be interpreted by specific pharmacophoric features selectivity model and binding modes in order to provide information for designing receptor-selective DPP-4 inhibitors.

The pharmacophore model described previously represents the contribution to the rational design of peptidomometic DPP-4 inhibitors. This pharmacophore contained one hydrophobic region, one positive ionizable region, one aromatic region and two hydrogen bond acceptor region. The successful explanation of structure activity relationships proves the efficiency of pharmacophore model to screen identify and predicted the activity of unknown molecules. This pharmacophore model was used to identify pharmacophore sites and predicts the activity of designed molecules. The alignments of pharmacophore features to designed molecules are shown in figure **3(i)**. The pharmacophore hypothesis showing distances between pharmacophoric sites and angles is depicted in Fig. **4.3(ii)**.The predicted activity and fitness score of designed molecules based on 3D- QSAR pharmacophore model are reported in Table **4.1**. Fitness score revels that all the designed compound fited and aligned with most of pharmacophoric features and explore good predicted activity.

Euclidean based applicability domain (AD) is calculated to ensure that the compounds of the external set are representative of the training set compounds used in model development. It is based on distance scores calculated by the Euclidean distance norms. At first, the normalized mean distance score for training set compounds are calculated and these values range from 0 to 1 (0=least diverse, 1=most diverse training set compound). Then normalized mean distance score for test set are calculated, and those test compounds with a score outside the 0 to 1 range are said to be outside the applicability domain. Fig. 4.4 justify that designed compound exhibited inside

the domain area covered by a training set compound that revels that designed compound are inside the applicability domain. These findings demonstrate that our pharmacophore is able to capture all of the essential features for an inhibitor interaction with the DPP-IV binding-site, which would explain why all of the assayed molecules show activity as DPP-IV inhibitors.
These findings demonstrate that our pharmacophore is able to capture all of the essential features for an inhibitor interaction with the DPP-4 binding-site, which would explain why all of the assayed molecules show activity as DPP-4 inhibitors.

DPP-4 selectivity of designed molecules with respect to DPP-2, DPP-8, and DPP-9 were predicted using previously reported HQSAR models shown in Table 4.2. Graphical Comparative studies of selectivity between compound taken in series for model development, Screen molecule and designed molecules are shown in graph A,B, C for all three models **(Fig. 4.4b-d)**. Overall, the designed 24 molecules were exhibited satisfactory prediction and selectivity as compare to azabicyclo series and screened piperazine molecules from 3D-QSAR models and HQSAR models. These predictions help in longer action of drug and reduce the side effect as severe toxic reaction, alopecia, thrombocytopenia, anemia and increased mortality. Finally, Designed and Synthesized 24 molecules contain three small hydrobhobic fragment cynopyrollidine, triazole and thiazole at S1 site and eight aromatic and hetroaromatic fragment at S2 site shown in figure **4.5**. There molecular properties are shown in table 4.3.

4.3.2 Docking Screening

Molecular docking simulations were performed for the screen the active hit from combinatorial library. A novel scoring function and docking protocol as Glide has been used to estimate protein-ligand binding affinities. Three different level of screening HTSV, SP and XP were performed in order to understand the enzyme-inhibitor key interactions that contribute to the most stable complex conformation. Finally, All designed 24 novel molecules were docked into the active site of DPP-4 in order to determine their putative binding mode using Extra precision mode (XP). The crystal structures demonstrated that the binding pocket of DPP-4 was located inside the center and consists of SI pocket, S2 pocket, catalytic triad Ser630-Asp708-His740, Tyr547, Glu205-Glu-206 and other residues**.** Most DPP-4 inhibitors contain a hydrophobic part tooccupy the SI pocket formed by residues Tyr631, Val656, Trp659, Tyr662, Tyr666 and

Val711. The S2 pocket is bounded by Ser209, Phe357 and Arg358.Previously reported that the piperazine includes an ideal geometry of two essential features required for a good affinity profile: a basic amine (protonated at physiological pH) and a hydrophobic feature.

Moreover, Result of electrostatic potential -2.66 to -4.31 also shows that –NH piperazine ring that common positive formal allows them to form ionic interactions with two of the binding residues in the EEloop pocket (i.e., Glu 205 and Glu206)(Table 4.4). The keto carbonyl group forms a hydrogen bond with Asn710 that, according to results shown in Figure 4.6.

Figure 4.6 shows the docked poses for **6a** and **6f** derivatives can be used to explain the structural basis of the expected increase in binding affinity. Remarkably, the XP GScores for these poses are in the -4.58 to -9.33 Kcal/mol range (see Table 4.4), therefore, the designed piperazine derivatives reported in Table are likely to exhibit nanomolar activity as DPP-4 inhibitors. As shown in Figure 4.6, the **6a** and **6f** derivatives usually maintained the most important protein-ligand interactions found for the designed core. Compound **6f** have highest docking score -9.33 shows one ionic interactions between the protonated amino groups of the ligands and Glu205 residues and cyno substitution of pyrollidine ring form non covalent interaction with Tyr 547, keto carbonyl group forms a hydrogen bond with Asn710 and benimidazole –NH forms hydrogen bond with Arg 358 of the receptors constitute are main essential interaction(Fig. 4.6righ panel).Additionally, Different substituents cynopyrollidine, thiazole and triazole at S1 bindinglocation also aid in increasing the protein-ligand binding affinity by enclosing the two sides of the corresponding ring in the hydrophobic protein environment in the S1 pocket.

Furthermore, all different substituents **(a-h)** at the S2 site are able to make hydrogen bonds and increase lipophilic nature either with the S2 pocket residue Arg358 or with Tyr 585 and Arg669.

Analysis of binding score of **6a-h**, **10a-h** and **14a-h**, respectively, revealed that receptors have two hydrophobic pockets small and large around the S2 site and the hydrophobic substituents of1to 8 bind to these pockets. Hydrophobic interaction of the substituents **(a-h)** played the key role in distinguishing selectivity and potency of the DPP-4 inhibitors **(Fig 4.7)**.Therefore, the substituents selected for the S1 and S2site by the combinatorial screen are able to form the intermolecular interactions with the S2 pocket that previous SAR studies with anti-diabetic drugs have shown to increase the affinity for the DPP-4 binding site.

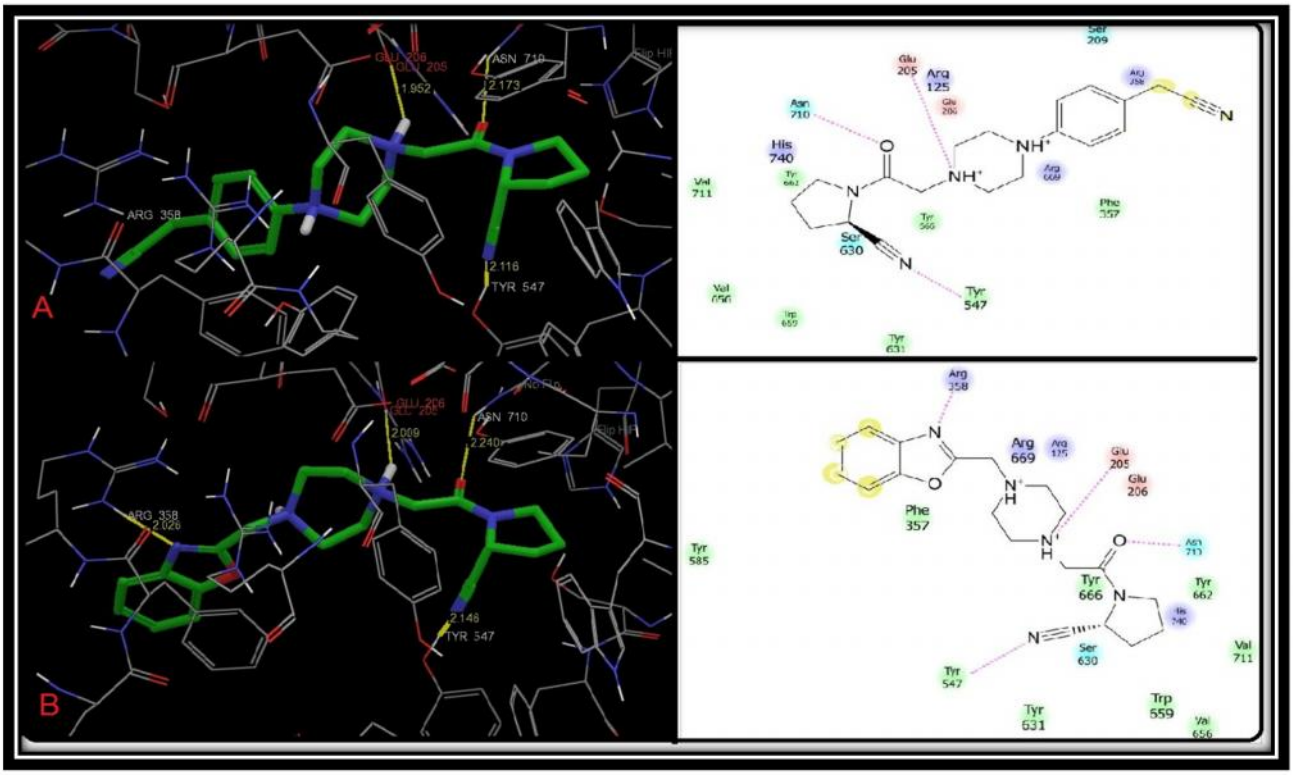

Figure 4.6 Hydrogen bonding interaction between compound (A) molecule **6a** (B) molecule **6f** and key amino acids of the active site (PDB: 1N1M). Right panels are two dimensional illustrations of the binding mode analyses. The H-bond interactions are depicted as yellow dotted lines, the H-bond length (Å) was labeled in the picture.

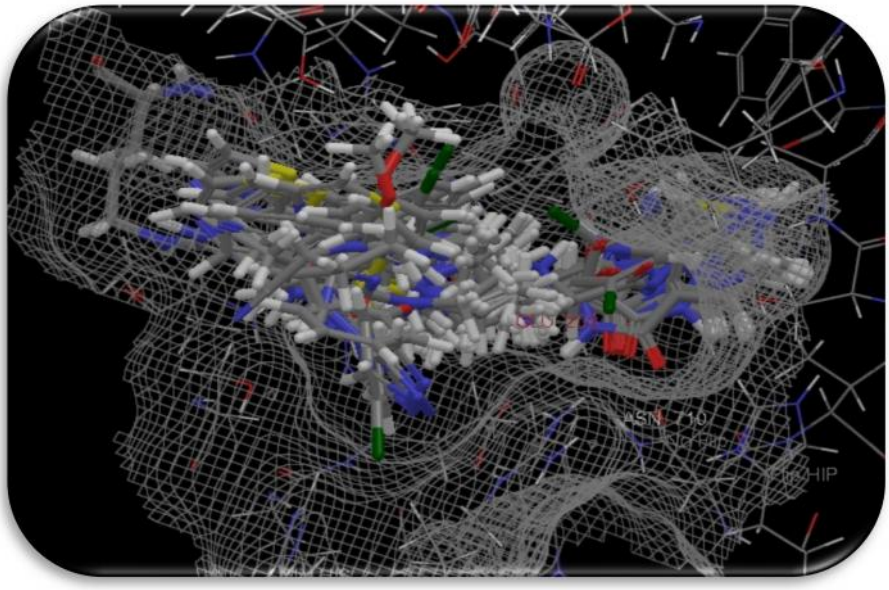

Figure 4.7 Docking alignment of all synthesized molecule in binding cavity

Tables 4.3 Molecular properties of designed and synthesized compounds

S.N.	Comp.	MW	ClogP	HBA	HBD	RB	PSA	Estate	MR	Polar
6a	SA01	337.42	0.845	3	0	5	74.37	57.83	100.02	40.18
6b	SA02	356.42	1.384	4	0	4	76.88	65.50	98.77	40.88
6c	SA03	357.84	1.340	3	0	4	74.37	60.11	98.91	40.31
6d	SA04	300.36	-0.289	4	0	3	76.36	50.17	84.97	33.99
6e	SA05	396.89	2.389	4	0	5	93.1	69.61	100.69	42.30
6f	SA06	353.42	1.619	4	0	4	76.61	57.50	97.44	41.14
6g	SA07	352.43	1.769	3	1	4	79.26	57.00	101.09	42.28
6h	SA08	380.44	0.509	4	1	5	96.33	64.00	105.78	44.75
10a	SB01	325.37	-1.11	4	1	6	90.08	56.00	95.14	39.03
10b	SB02	344.37	-0.580	5	1	5	92.59	63.67	93.89	39.74
10c	SB03	345.79	-0.625	4	1	5	90.08	58.28	94.03	39.16
10d	SB04	288.31	-2.52	5	1	4	92.07	48.33	80.09	32.84
10e	SB05	384.84	0.423	5	1	5	108.81	67.78	95.81	41.15
10f	SB06	341.37	-0.34	5	1	5	92.32	55.67	92.56	39.99
10g	SB07	340.38	-0.195	4	2	5	94.97	55.17	96.21	41.13
10h	SB08	368.39	-1.454	5	2	5	112.04	62.17	100.90	43.60
14a	SC01	341.43	1.31	3	1	6	100.5	54.50	96.47	41.87
14b	SC02	360.43	1.849	4	1	5	103.01	62.17	95.22	42.57
14c	SC03	361.85	1.805	3	1	5	100.5	56.78	95.35	42.00
14d	SC04	304.37	0.175	4	1	4	102.49	46.83	81.42	35.67
14e	SC05	400.90	2.854	4	1	5	119.23	66.28	97.14	43.99
14f	SC06	357.43	2.084	4	1	5	102.74	54.17	93.88	42.83
14g	SC07	356.45	2.234	3	2	5	105.39	53.67	97.54	43.97
14h	SC08	384.46	0.974	4	2	5	122.46	60.67	102.22	46.43
Vildaglaptin		303.44	0.692	5	2	4	76.13	60.8	81.67	32.37
Saxaglaptin		315.41	-0.252	5	3	3	90.35	68.3	8.16	33.66

Tables 4.4 Docking interaction results of designed and synthesized compounds

ligand	GScore	Lipophilic EvdW	Electro	HBond
SA01	-8.92	-1.56	-4.31	-1.39
SA02	-7.75	-1.59	-2.76	-1.97
SA03	-7.6	-1.65	-2.73	-1.6
SA04	-7.51	-1.43	-2.7	-1.7
SA05	-7.62	-1.71	-2.78	-1.62

SA06	-9.33	-1.52	-4.31	-1.73
SA07	-8.27	-1.52	-2.96	-2.19
SA08	-7.97	-1.88	-3.32	-1.25
SB01	-6.51	-1.29	-4.43	-0.7
SB02	-5.86	-1.24	-2.97	-1.14
SB03	-7.27	-1.4	-4.11	-1.5
SB04	-4.58	-1.18	-2.66	-0.75
SB05	-5.62	-1.48	-2.65	-1.34
SB06	-7.37	-1.21	-4.46	-1.62
SB07	-7.24	-1.8	-3.33	-0.82
SB08	-9.11	-2.01	-3.01	-2.62
SC01	-6.54	-1.6	-4.37	-0.7
SC02	-5.5	-1.96	-2.74	-0.82
SC03	-8.53	-1.36	-4.18	-1.27
SC04	-5.29	-1.69	-2.71	-0.74
SC05	-5.67	-1.94	-3.27	-0.75
SC06	-7.13	-1.95	-2.58	-0.95
SC07	-7.41	-1.97	-3.21	-0.86
SC08	-9.08	-2	-3.44	-2
Sitaglaptin	-5.07	-1.37	-1.03	-0.88

4.3.3 ADME studies

Prediction of ADME parameters prior to experimental studies is one of the most important aspects in the drug discovery and development of drug molecules. Screened hits were studied using Qikprop (Schro¨dinger, LLC, NewYork, USA). Forty four physically descriptors and pharmaceutically relevant properties of synthesized compounds were analyzed using Qikprop, among which significant descriptors that were reported are required for predicting drug-like propertiesof molecules. These properties were Molecular weight (mol_MW) (150–650), Octanol/water partition coefficient (log P o/w) (-2 to 6.5) (Table 4.3), Aqueous solubility (QPlog S) (-6 to 0.5) Percent human oral absorption ([80 % is high,\25 %are poor) (table 4.5).

Further, Volume of distribution (Vd)., % plasma protein binding, oral bioavability and drug likeness were calculated by ACD ILab tool. Toxicity in regards to mutagenic, tumorigenic,

irritant and Reproductive effect were estimated by Osiris property explorer and mentioned in table 4.6.

Tables 4.5 ADME Properties of final compounds

Comp	LogS	% human oral absorption	Vd(L/KG)	%PPB	Oral bioavailability	Druglikness
SA01	-1.999	54.849	1.37	58.24	0.69	0.02
SA02	-1.545	62.048	1.28	50.01	0.698	0.92
SA03	-2.409	58.329	1.59	64.63	0.698	1.89
SA04	-1.571	64.15	0.97	53.99	0.698	4.55
SA05	-0.793	51.372	1.37	66.98	0.772	3.49
SA06	-0.276	52.15	1.03	48.65	0.698	2.97
SA07	-1.441	47.506	1.51	39.25	0.698	3.17
SA08	-1.166	38.356	2.11	31.38	0.722	3.84
SB01	-2.566	57.594	1.34	47.87	0.722	-0.32
SB02	-1.157	60.041	1.15	30.18	0.772	4.71
SB03	-2.605	54.814	1.37	47.71	0.698	1.72
SB04	-0.773	59.811	0.69	44.32	0.698	7.44
SB05	-1.081	53.56	1.23	69.43	0.772	6.22
SB06	0.247	44.348	1.31	54.68	0.698	7.42
SB07	-0.577	46.523	1.42	42.10	0.698	7.63
SB08	-0.452	38.308	1.26	38%	0.698	7.92
SC01	-4.113	71.261	1.95	85.03	0.772	-0.39
SC02	-2.487	76.423	1.48	71.03	0.772	8.45
SC03	-3.317	73.271	1.29	64.43	0.698	1.56
SC04	-2.22	76.27	0.72	69.43	0.698	8.64
SC05	-2.344	70.424	1.46	71.43	0.772	4.53
SC06	-1.328	65.827	1.24	59.53	0.698	6.08
SC07	-1.584	67.298	1.41	56.43	0.698	7.46
SC08	-1.542	51.067	1.26	48.65	0.698	7.71

Table 4.6 insilico Toxicity Data of final compounds

Comp	Mutagenic	Tumorigenic	Irritant	Reproductive effect
6a	Green	Green	red	yellow
6b	Green	Green	Green	Green
6c	Green	Green	Green	Green

6d	Green	Green	Green	Green
6e	Green	Green	Green	Green
6f	Green	Green	Green	Green
6g	Green	Green	Green	Green
6h	Green	Green	Green	Green
10a	Green	Green	red	yellow
10b	Green	Green	Green	Green
10c	Green	Green	Green	Green
10d	Green	Green	Green	Green
10e	Green	Green	Green	Green
10f	Green	Green	Green	Green
10g	Green	Green	Green	Green
10h	Green	Green	Green	Green
14a	Green	Green	red	yellow
14b	Green	Green	Green	Green
14c	Green	Green	Green	Green
14d	Green	Green	Green	Green
14e	Green	Green	Green	Green
14f	Green	Green	Green	Green
14g	Green	Green	Green	Green
14h	Green	Green	Green	Green

4.4 Conclusion

The previously reported pharmacophore model, HQSAR selectivity models and a 'lead-like' screening hit inspired the development of a series of piperazine-constrained DPP-4 inhibitors. A novel series of DPP-4 inhibitors with excellent potency and selectivity over DPP-2, DPP-8 and DPP-9 has been discovered by insilico method. These novel piperazine derivatives were design, synthesized and evaluate for DPP-4 inhibitory activity.

The docking results and predicted activities were in accordance with the biological activity data. Thus, peptidomimetic based cyanopyrrolidine derivatives as potent, selective and long acting DPP-4 inhibitors for an effective treatment of T2DM.Future optimization of piperazine derivatives can lead to the discovery of new potent compounds.

4.5 References

1. Ghate M., Jain S. V., Fragment based HQSAR modeling and docking analysis of conformationally rigid 3-azabicyclo [3.1.0] hexane derivatives to design selective DDP-4 inhibitors, Lett. drug design discov.. 11(2), 184-185
2. Ghate M., Jain S. V., Atom based Pharmacophore modeling, CoMFA/CoMSIA based 3D-QSAR studies and lead optimization of DPP-4 inhibitors for the treatment of type 2 diabetes. Med Chem Res. DOI: 10.1007/s00044-014-0923-2.
3. Jain S. V., Bhadoriya K. S., Bari S. B., Sahu N. K., Ghate M.**,** Discovery of potent anticonvulsant ligands as dual NMDA and AMPA receptors antagonists by molecular modelling studies, Med Chem Res, 2012, 21,3465-*3484*
4. VLife MDS 3.5 (2008) Molecular design suite. Vlife Sciences Technologies Pvt. Ltd., Pune. www.vlifesciences.com.
5. Singh S. K., Manne N., Pal M., Synthesis of (S)-1-(2-chloroacetyl)pyrrolidine-2-carbonitrile: A key intermediate for dipeptidyl peptidase IV inhibitors, Beilstein Journal of Organic Chemistry 2008, 4, 20
6. Bali A., Sharma K., Bhalla A., Bala S., Reddy D., Singh A., Kumar A., Synthesis, evaluation and computational studies on a series of acetophenone based 1-(aryloxypropyl)-4-(chloroaryl) piperazines as potential atypical antipsychotics, European J. Med. Chem., 2010, 45, 2656-2662.
7. Gu S. J., Lee J.K., Pae A N., Chung H J., Rhim H., Han S Y., Min S. J.,Cho Y. S., Synthesis and biological evaluation of 1,4-diazepane derivatives as T-type calcium channel blockers, Bioorganic & Medicinal Chemistry Letters, 2010,20, 2705–2708.
8. Sreena K, Ratheesh R, Rachana M, Poornima M, Shyni C. Synthesis and Antihelmintic Activity of Benzimidazole Derivatives HYGEIA, Vol.1, No.1/March-Aug, 09
9. Ullapu P. R., KuS. J., Choi Y. H., Park J., Han S.Y., Baek D. J., Lee J., Pae A. N.,. Min S. J, Cho Y.S., Synthesis and Biological Evaluation of 1-Heteroarylmethyl 1,4-Diazepanes Derivatives as Potential T-type Calcium Channel Blockers, Bull. Korean Chem. Soc. 2011,32, 83063.
10. Li F., Feng Y., Meng Q., Li W., Li Z., Wang Q.,Tao F., An efficient construction of quinazolin-4(3H)-ones under microwave irradiation, ARKIVOC ,2007 (i) 40-50.